



Developing GIS-based earthquake loss model: a case study of Baqiao District, China

Yixin Zhang^{1,2} · Shansuo Zheng^{2,3} · Longfei Sun⁴ · Li Long² · Wei Yang⁵ · Lei Li^{2,3}

Received: 14 November 2019 / Accepted: 30 December 2020 / Published online: 4 February 2021
© The Author(s), under exclusive licence to Springer Nature B.V. part of Springer Nature 2021

Abstract

Large earthquakes frequently occurred and caused substantial damage and losses in Chinese densely populated urban areas. It is worth clarifying that the existing earthquake loss assessment tools in China do not consider its special characteristics (e.g., tectonics, geology and building inventory). In this paper, an integrated framework for earthquake loss assessment in China is proposed and a geographic information system (GIS)-based system, referred to as China Earthquake Disaster Loss Assessment System, is developed. The individual building is considered as the basic geographical unit and described in three levels (i.e., basic attributes, structural performance parameters, and functional parameters). A three-step data collection method is proposed, and the mobile GIS-based field collection tool is developed. A broad, reasonable, and upgradeable building typology is then presented for the seismic fragility assessment of building blocks. A new economic loss model and casualty model are also presented by considering the characteristics of economics and population. The proposed methodology is implemented in Baqiao District, and the estimation of economic losses and casualties under a scenario earthquake is discussed, which can provide information for urban disaster risk assessment and mitigation.

Keywords Earthquake loss assessment · Data collection · GIS · Building typology · Seismic fragility · Economic loss model · Casualty model

✉ Yixin Zhang
zhangyixin@live.xauat.edu.cn

✉ Li Long
1152684330@qq.com

¹ College of Civil Engineering, Huaqiao University, Xiamen 361021, China

² School of Civil Engineering, Xi'an University of Architecture and Technology, Xi'an 710055, China

³ Key Lab of Structural Engineering and Earthquake Resistance, Ministry of Education (XAUAT), Xi'an 710055, China

⁴ Country Garden Company, Xi'an 710055, China

⁵ RBS Architecture Engineering Design Associates, Shanghai 200063, China

1 Introduction

Earthquake disasters have been identified as a serious threat to human development, and a challenge to earthquake prevention (Ahmad et al. 2014; Haldar et al. 2013). China, located in the joint of the Circum-Pacific seismic belt and Eurasian seismic zone, is one of the most seismically active regions in the world (Hu 1990). Due to its dynamic tectonic characteristics, China is exposed to the highest seismicity risk. Recently, major earthquakes have occurred and caused severe damage and losses in some densely populated urban areas, especially in highly developed zones with structures vulnerable to earthquakes (Coburn and Spence 2003; Haldar et al. 2013; Lin et al. 2012; Xu et al. 2014). For instance, the 2008 Wenchuan earthquake caused 845.1 billion RMB in direct economic losses and more than 87,000 deaths, and the 2010 Yushu earthquake killed more than 2698 people and caused economic losses over 12.5 billion RMB. Considering the previous seismic disasters, the main reason underlying these losses is lack of well-planned preparedness activities in the country, which failed to consider the regional characteristics of structural performance and socio-economic level (Ahmad et al. 2014; Gong et al. 2015). As a vast area with diversity of economy and culture, potential threats in China also increased its challenges for disaster prevention and mitigation. The deficiencies and challenges include the following. (1) The structure type, seismic performance, and quantity of buildings vary from region to region, with high density in southeast coastal cities and low density in northwest cities of China. Masonry and adobe structures with poor seismic resistance performance (e.g., lower fortification level and poor construction without sufficient special details for ductile response), are found primarily in the Midwest rural areas, which have experienced a lower level of economic development (Gong et al. 2015; Wang 2008). (2) The new normal in China is urbanization. Statistics show that at the end of 2014, the mainland urban population was 749.16 million, 54.77% of the total population (NBSPRC 2015). With the high density and uneven distribution of people, the majority of low-income people live in older buildings or self-constructed buildings, mostly without code-compliant seismic design (Gong et al. 2015). The potential consequences including casualties and monetary losses would be immeasurable if earthquakes were to occur.

Earthquake loss assessment in China first began after the 1976 Tangshan earthquake. Loss assessment methodologies were achieved, especially in the early 1990s (Gao et al. 1989; Yin 1995). Earthquake loss assessment exercises mainly contain earthquake damage prediction, earthquake emergency response, and earthquake site disaster loss assessment (Sun et al. 2012). Earthquake damage prediction is mainly undertaken in the pre-earthquake period, providing estimation consequence for policy makers to guide disaster preparedness. As a vital work during earthquakes, earthquake emergency response can provide emergency relief for decision-makers and reduce casualties and economic losses. Earthquake site disaster loss assessment involves field investigation after earthquakes, which can assess the detailed consequent losses and provide guides for reconstruction. All exercises have made a great contribution to the work of earthquake loss assessment, especially in 2008 Wenchuan earthquake. China has experienced many destructive earthquakes. However, the existing earthquake loss assessment in China does not account for its special characteristics, such as the vulnerability of structures and the distribution characteristics of population and economy, which affects the accuracy of earthquake loss assessment.

The main objective of the present research work is to develop an integrated framework by combining the existing methodologies of China. At the same time, some research work is attempted to improve the overall methodology, which includes the following: a new data

collection method is devised using a mobile Geographic Information System (GIS) -based field collection tool that can effectively collect detailed building inventory; a hierarchical, detailed, and extensible building typology is proposed, which can consider the differences in structural performance; and a new economic loss model and casualty model are developed for use on individual buildings. Then, the integrated framework is embedded into the China Earthquake Disaster Loss Assessment System (CEDLAS) for use in different assessment phases, i.e., pre-, intra-, and post-earthquake periods. Components of the CEDLAS are discussed here including the seismic hazard analysis, inventory, fragility functions, and loss assessment. Baqiao district is adopted as a case study and the loss assessment is carried out to provide useful information for urban disaster risk assessment and mitigation.

2 Earthquake loss assessment framework

2.1 General framework

The vision of the earthquake loss assessment methodology is to provide emergency relief and rehabilitation guidance for the decision-makers after earthquakes, and also to guide the planning and mitigation of earthquake disasters and earthquake insurance in seismic risk assessment (Federal Emergency Management Agency, FEMA 1997). Various studies have been conducted with earthquake loss assessment methodologies (Choun and Elnashai 2010; Duzgun et al. 2011; FEMA 1997), and also some unique tools for decision-makers to assess the impact have been developed, e.g., HAZUS-MH (FEMA 2012a, b), SELINA (Molina et al. 2010), OpenQuake (Pagani et al. 2014; Silva et al. 2014), MAEViz (2018), and SYNER-G (<http://www.vce.at/SYNER-G/>). Unfortunately, due to the differences in tectonics, geology, and building inventory, the current methodologies or tools may not apply for China. In order to consider the differences, three key points are summarized as below.

1. New and efficient techniques should be developed for acquiring useable building inventories in a large urban areas, an advanced data collection method and procedure are presented.
2. In general, building-specific information cannot be easily obtained from the raw inventory data (SVAPG 2013). Therefore, it is necessary to adopt a broad, reasonable, and upgradeable building typology for a large number of buildings.
3. The distribution of wealth, population, and external environment can vary in different urban areas. The loss model is a complex, dynamic, and cross process, which should take the different economic status among urban areas into consideration.

By addressing the above issues, this paper presented an integrated, flexible, extensible loss assessment framework which includes seismic hazard analysis, inventory, fragility, physical damage, and loss assessment (direct economic and casualty) as shown in Fig. 1. As it can be seen that modules are interdependent with output of some modules acting as input to others. In seismic hazard analysis module, both China probabilistic seismic hazard assessment (CPSHA) and deterministic seismic hazard analysis (DSHA) methods are used to assess seismic hazard of regional areas. The output of mapping peak ground acceleration (PGA) and spectral acceleration (S_a) can be used as inputs in physical damage. Inventory is a major and essential phase in loss estimation

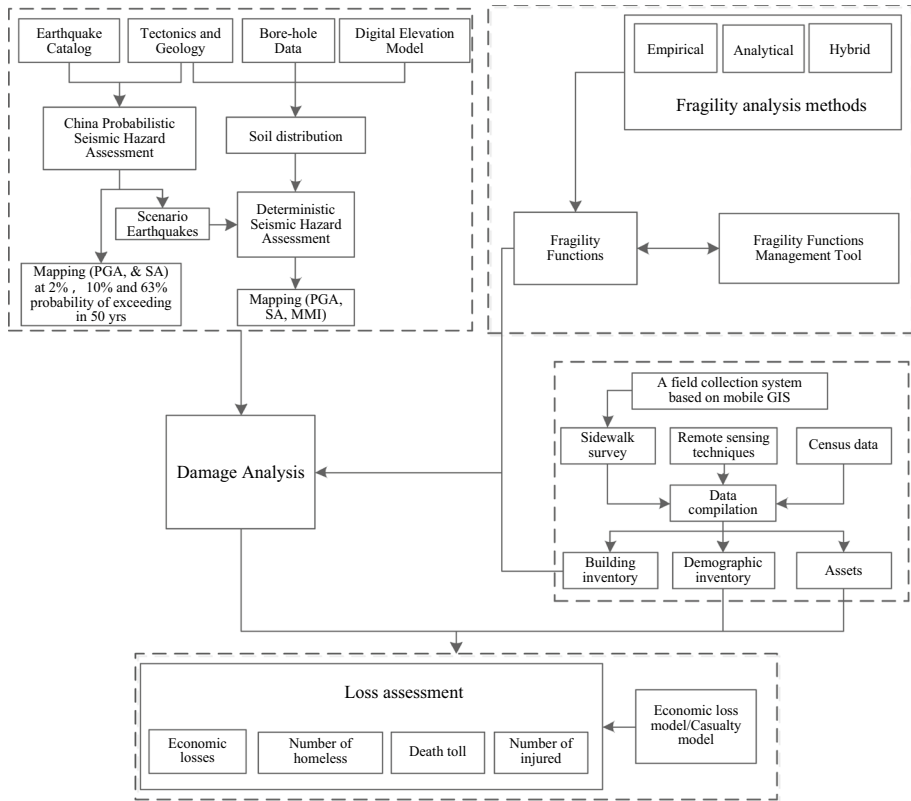


Fig. 1 Architecture of the proposed integrated framework

for a group of buildings and is also a collection set of information (e.g. building characteristics, construction practice, occupancy, and other social and economic aspects). In the module, the data are collected by multiple approaches and processed as inputs to others. Fragility quantifies the properties of structures to be damaged by specified ground motions. The fragility functions have been obtained as the basic input to physical damage. The loss assessment module is the combination of the above modules. The direct economic loss and number of casualties can be estimated for policy-makers to guide the planning. The relationship between modules is illustrated in Fig. 2.

All components are refined and tailored to proposed GIS-based system CEDLAS to achieve a seamless integration and to arrive at an operational system. The system is established based on C/S architecture with .Net as the development platform and ArcGIS Engine components as the key technology. The source code is written in C# language with the integrated development environment. The technical sides of developing the system can be referred to a companion paper (Long et al. 2020), including plugin management, view definition, and interface design. Core source codes are also provided.

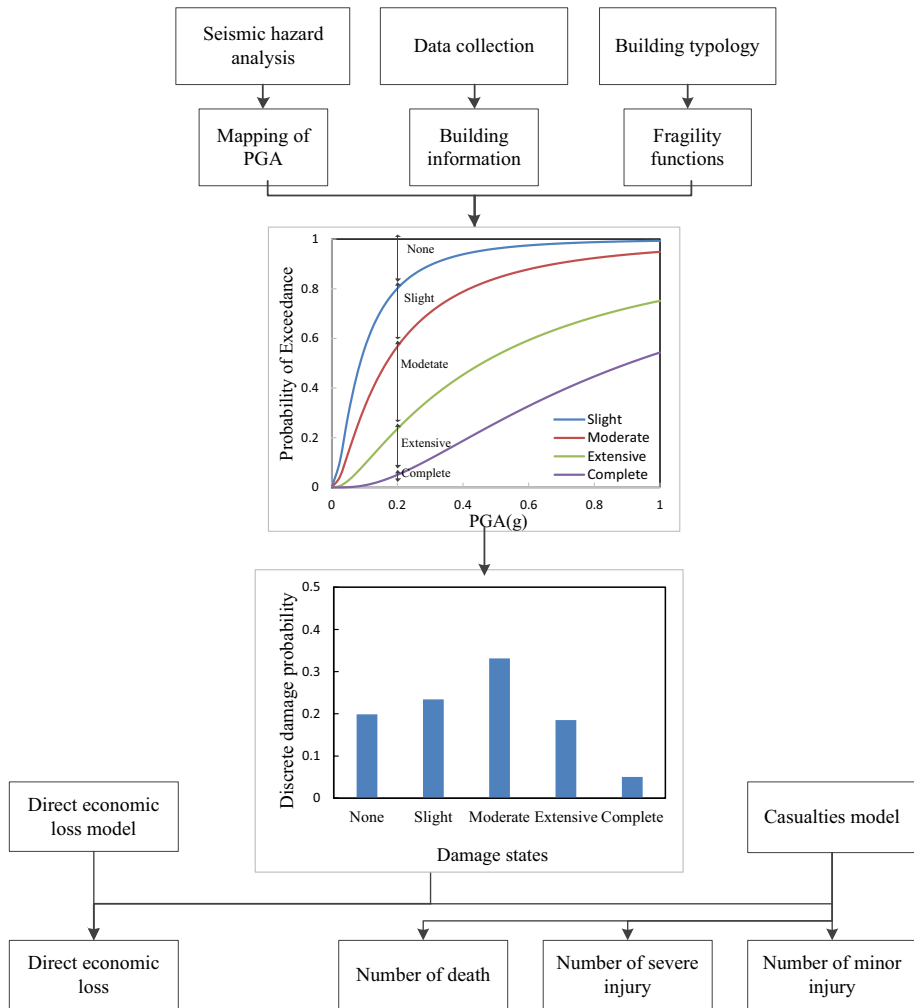


Fig. 2 Methodology of the proposed framework

2.2 Uncertainties of earthquake loss assessment framework

Each component in the proposed framework carries associated uncertainties that can be propagated through the analysis (Ahmad et al. 2014). In general, uncertainties in the earthquake loss assessment can be categorized into two groups, i.e., aleatoric and epistemic. Aleatoric uncertainty is related to the inherent randomness of limited data. Epistemic uncertainty is associated with a lack of knowledge and assumptions in modeling techniques, which can generally be reduced with additional information and more comprehensive analysis (Ellingwood and Wen 2005; Jeon 2013). In this paper, the uncertainties of ground motion attenuation models and structural fragility functions are considered. The logic tree method is used to consider the uncertainty of ground motion attenuation models by attaching a weight value for each model. In order to access the

earthquake loss, the classical structures are defined. The uncertainties in the earthquake and structure are combined by variety of incremental dynamic analysis (IDA).

3 Components of earthquake loss assessment framework

3.1 Seismic hazard analysis

The main goal of seismic hazard analysis is to estimate ground motions and return period at the site or in a region (Liu et al. 2013). Recent research shows that DSHA and probabilistic seismic hazard analysis (PSHA) are the most frequently used methods (Wang and Taheri 2014). DSHA estimates ground motion from a worst-case earthquake magnitude and location by considering a small number of scenarios (Liu et al. 2013; Wang and Taheri 2014). Conventional DSHA has the advantage of having a clear physical and statistical meaning; however, the temporal characteristics of an earthquake are not considered. PSHA aims to quantify the uncertainties related to earthquake occurrences with respect to time, location, space, and magnitude, and combine them to produce an explicit description of the distribution of future shaking that may occur at a site (Baker 2008; Cornell 1968; McGuire 2008). By considering spatially and temporally inhomogeneous seismic activities in China, a modified PSHA method (CPSHA) was proposed and implemented into the seismic hazard map of China (National Standard of People's Republic of China, NSPRC 2015). The tri-class seismic source model in CPSHA consists of the seismic province, the background seismicity zone and the tectonic features zone (Pan et al. 2013). In the framework, the CPSHA method is used to determine seismic hazard assessment in regional areas. Mapping of PGA and S_a (e.g., 2% in 50 years and 10% in 50 years) can be described, and the magnitude and location of a potential earthquake (the worst-case earthquake) can be estimated. Furthermore, the DSHA method is used to estimate the seismic hazard analysis of local regions by considering the worst-case earthquakes and site conditions. In addition, it is worth mentioning here that ground motion attenuation model has a significant influence on seismic hazard analysis. In order to consider the geotectonic characteristics of China, the models are established in accordance with the models used in the western United States due to the limitation of ground motion recorders in China. In this paper, the ground motion attenuation models for the New Seismic Hazard Map of China by Yu et al. (2013) and other research on special regions of China (Fan et al. 2011; Yu and Wang 2003) are all integrated into the module.

3.2 Inventory

The accuracy of the estimation results depends on the data used for the analyses, including structure type, occupancy, building height, construction year, population and content value (Bal et al. 2008; Jaiswal et al. 2010; Mansouri et al. 2010; Mansouri and Amini-Hosseini 2014; Sahar et al. 2010). Nevertheless, due to the wide coverage and large number, it is difficult to obtain useable building inventory. Two significant technical challenges are faced here: (1) how to describe the inventory that can be suitable for earthquake loss assessment and (2) how to develop an advanced data collection method that can be used for data acquisition and inventory updates.

In practice, for the sake of efficiency, a building block or city district is mainly used as the basic geographical unit in some risk estimation software tools (FEMA 2012a, b;

Molina et al. 2010). However, in reality, buildings consist of collective sets of information, varying widely in characteristics and numbers. In order to depict the inventory in detail, a unique hierarchical description method is proposed here. The description of individual buildings is divided into three levels, as shown in Table 1.

As mentioned previously, individual buildings vary widely in characteristics. However, this information is scattered in different sectors (e.g., the civil affairs department, public security department and statistics department) and presents huge data collection challenges. The methods in data collection can be categorized into three groups: census data, ground survey, and field data and remote sensing techniques. As basic datasets, census data represent fundamental inputs for vulnerability assessment (JRC 2013; Ketner 2008). The procedure of a field survey may be divided into two groups: paper forms and hand-held equipment-based forms (Annunziato et al. 2010; FEMA 2002; IDCT 2011). The techniques of GIS, remote sensing, and multi-source imaging are applied for rapid data collection (Wieland et al. 2012; Spence 2011). Based on existing methods, a data collection procedure is proposed with neighborhood community or administrative village as the basic geographical unit to collect and summarize the data. The data collection has three steps (see Fig. 3).

As shown in Fig. 3, step one is the preparation before data collection, including the acquisition and geo-referencing of high-resolution remote sensing images, communicating with local government leaders, consulting the statistical reports and formulating the collection scheme, and training the collectors. Step two is sidewalk collection using two approaches: paper form-based and mobile GIS-based. The first approach is time-consuming but suitable for non-professional collectors. In order to improve the efficiency and accuracy, a mobile GIS-based field collection system is also applied. The approach can quickly locate the individual building position and efficiently interact with the basic data platform (see Fig. 4). Step three is the inside data processing, including the vector and matching treatment for the first approach results, checking data and uploading to a basic data server. To build an extensible basic data platform, the model combines ArcGIS with Geodatabase, which can integrate spatial data (e.g., administrative divisions, buildings, and roads) and attribute data into the geodatabase model (ESRI 2010).

Some problems arise in data collection. Due to the diversity of information, some parameters cannot be obtained directly, such as floor area, occupants and content value. Multiple approaches are combined and conducted to cope with the issues in our research work. Census data and statistical reports are consulted to obtain the raw data such as functional parameters; in addition, some parameters can be obtained from the existing building design drawings. Under the assistance of local government, various building design drawings are gathered and consulted, which may obtain reliable information. However, a field survey must be conducted due to the limitation of resources. Thus, some equipment is needed in field surveys, such as measuring tape and a laser telemeter. For instance, a data collection method for the floor area and others is shown in Fig. 5.

3.3 Fragility functions for structures

Seismic fragility functions describe the probability associated to a given component or building of exceeding predefined damage limit states at the given level of ground shaking. Fragility of buildings implies in macro-seismic intensity scales is commonly used for the earthquake disaster prediction in nation scale. However, when using this method, it is difficult to show the seismic performance of buildings with different qualitative characteristics

Table 1 Description of individual building levels

Levels	Sub-category	Description
Basic attribute	Unique ID	This is the intuitionistic description of individual buildings, including the location, name, pictures, architectural drawings and file saving location. This can be obtained from sidewalk collection, remote sensing images and Census data
	Building name	
	Environmental characteristic	
	Latitude	
	Longitude	
	Building pictures/videos	
	Documents	
	Collector description	
	Material type	
	Load resisting system	
Structural performance parameters	No. of stories (upper/underground)	The seismic performance of buildings refers mainly to the parameters (structure type, building height, design code), which have major impact on structural fragility analysis. This can be obtained from sidewalk collection and statistical reports
	Building height	
	Construction year	
	Seismic design code	
	Seismic precautionary intensity	
	Roof type	
	Irregularity	
	Condition of construction	
	Occupancy	
	Hierarchy of criteria	
Functional parameters	Floor area	This is an essential parts for loss assessment (e.g., decoration level, occupancy, content value and population). This can be obtained from sidewalk collection and statistical report
	Cost of construction	
	Occupants	
	Content value of indoor	
	Content value of outdoor	
	Decoration level	

(such as building height, seismic design code, and construction year). In general, obtaining fragility functions for buildings in Chinese urban areas currently faces two significant technical challenges: (1) proposing a reasonable and upgradeable building typology for a large number of buildings and (2) carrying out fragility analysis for different building typologies.

3.3.1 Building typology

With the requirement of seismic loss estimation, a number of studies in building typology have been conducted in earthquake-prone areas (ATC-13 1985; Brzev et al. 2013; FEMA 1997; Ptilakis and Argyroudis 2014). Several parameters were taken into account, such as the material of construction, building height, structural frame system, and other qualitative characteristics. For instance, HAZUS developed by FEMA considered construction material, load resisting system, and building height (FEMA 2012a, b). GEM (2013) developed a refined taxonomy which considers most general building characteristics (e.g., roof, hazards, and occupancy), and main detailed characteristics (e.g., construction material, structural element, lateral load resisting system, and height). Furthermore, some new building typologies were also employed related to local building stocks (Mansour et al. 2013; Mansouri and Amini-Hosseini 2014). However, the typology cannot fully used for Chinese buildings due to the differences in the seismic design code of buildings, construction standard as well as local characteristics.

Considering the difficulty in obtaining detailed building-specific information from the raw inventory data, it is necessary to propose a broad building typology for China. Based on the Chinese Code for Seismic Design of Buildings (CCSDB) (NSPRC 2010), a hierarchical, detailed, and extensible building typology is proposed as shown in Table 2. Building categorization parameters are described below.

1. Material Type

Based on the construction material, the buildings are generally classified into four types which are wooden structure/masonry/reinforced concrete/steel, respectively.

2. Structural framing system

The choices of structural framing system are determined by construction material, building height and seismic design code. The types of structural framing system are divided into five classes, including wall system (stone masonry/adobe/burnt clay brick/block masonry), moment resisting frame, shear wall structure, frames with walls (cast-in-place concrete shear walls/masonry infill walls/un-reinforced masonry infill walls), and braced frame.

3. Height level

Building height is a vital factor in determining the natural period of a building and its vulnerability. Various classifications for height level have been proposed in assessment methodology and codes (NSPRC 2010), hence, the height level of buildings are classified into four categories according to the number of stories. They include Low-rise (1–3), Mid-rise (4–9), High-rise (10–33 and < 100 m), Super high-rise (33+ or > 100 m).

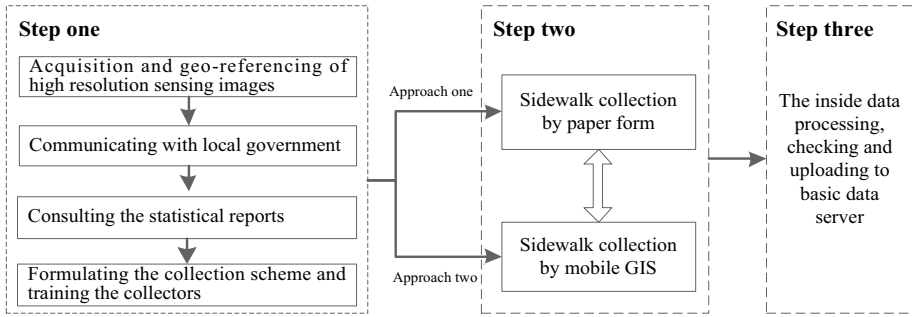


Fig. 3 Description of data collection procedures. From left to right: preparation step, sidewalk collection step, inside data processing step



Fig. 4 Screen shot of the mobile GIS-based field collection system

4. Irregularities

The horizontal and vertical irregularities in buildings have a great influence on the seismic performance of buildings. In general, if a building’s mass center is not consistent with its stiffness center, the torsional action may intensify damage. Horizontal and vertical irregularities used here are defined in chapter 3.4 and 3.5 of CCSDB (NSPRC 2010).

5. Code level

The level of seismic design greatly determines the seismic performance of existing buildings (Ahmad et al. 2018). Based on the evolution of CCSDB (NSPRC 1979, 1989, 2001, 2010), building classification is divided into four stages: Pre-code (buildings constructed before 1978 or constructed without seismic code); Low-code (buildings constructed from 1978 to 1989); Moderate-code (buildings constructed from 1989 to 2001); High-code (buildings constructed after than 2001).

6. Seismic precautionary intensity (SPI)

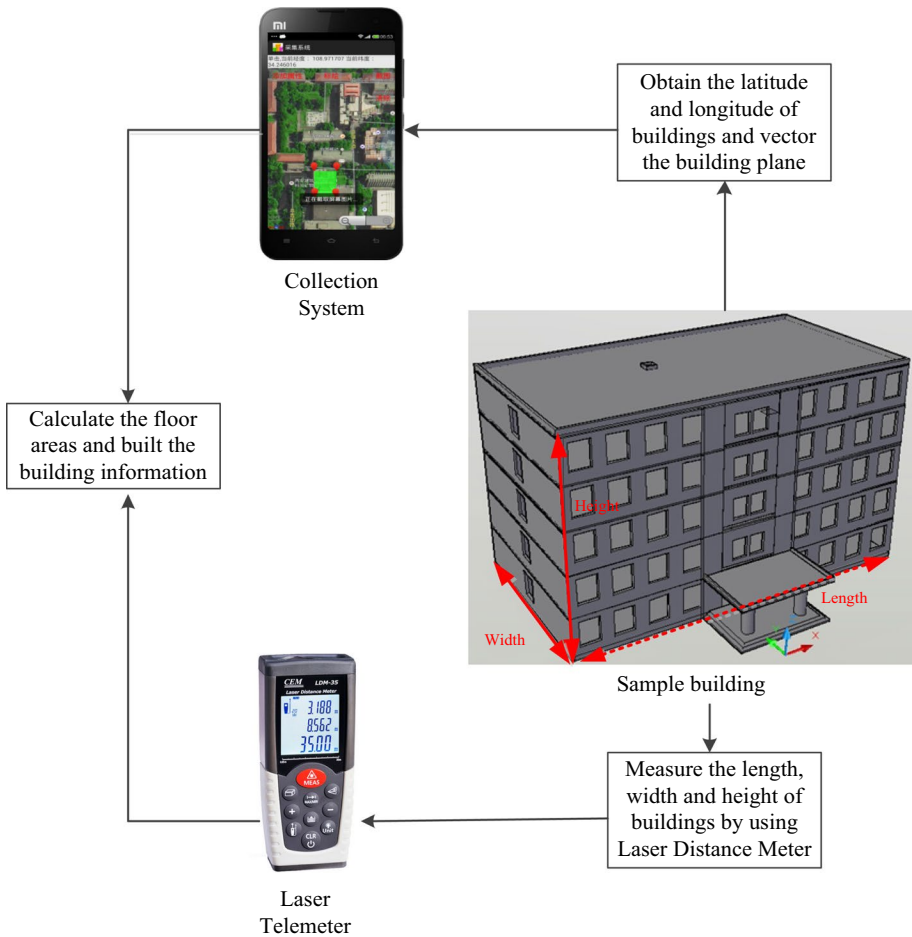


Fig. 5 Data collection method for the floor area and others

The seismic precautionary intensity in buildings is divided into six types as defined in GB 18306-2015 (NSPRC 2015) and GB 50011-2010 (NSPRC 2010). It is evident from past fatal earthquakes around the world that the existence of vulnerable buildings in high intensity areas has caused the highest number of fatalities. This is VI (0.05 g), VII (0.10 g), VII (0.15 g), VIII (0.20 g), VIII (0.30 g), IX (0.40 g).

7. Current state of the building

Research shows that the current state of the building would influence the structural damage when earthquake occurred, especially for the case of the aged buildings under low seismic intensity (e.g., VI, VII). Therefore the current state of the building is divided into five types: Buildings without structural damage; Buildings with slight structural damage; Buildings with moderate structural damage and in need of repair; Buildings with severe structural damage and in need of reinforcement; Dangerous buildings.

Table 2 Proposed building typology

Material	Building typology	Code	Height level	Irregularities		Code level	SPI	Building actuality
				Horizontal	Vertical			
Masonry (M)	Adobe walls	A	Low-rise	Regularities/irregularities	Regularities/irregularities	Pre-code; Low-code; Moderate-code; High-code;	VI (0.05 g) VII (0.10 g) VII (0.15 g) VIII (0.20 g) VIII (0.30 g) IX (0.40 g)	Intact buildings; Buildings with slight structural damage; Buildings with moderate structural damage and in need of repair; Buildings in need of reinforcement; Dangerous buildings
	Stone masonry walls	ST	Low-rise					
	Unreinforced burnt clay brick masonry	UBM	Low-rise					
	Unreinforced concrete block masonry	UCM	Low-rise					
	Reinforced burnt clay brick masonry	RBM	Low-rise					
	Reinforced concrete block masonry	RCM	Mid-rise Low-rise					
	Masonry walls with bottom-frame	MBF	Mid-rise Low-rise					
	Masonry walls with inner-frame	MIF	Mid-rise Low-rise					

Table 2 (continued)

Material	Building typology	Code	Height level	Irregularities		Code level	SPI	Building actuality
				Horizontal	Vertical			
Concrete (C)	Moment resisting frame	C1	Mid-rise					
	Frame with Cast-in-Place Concrete Shear Walls	C2	High-rise					
				Mid-rise				
	Shear walls	C3	High-rise					
			Mid-rise					
	Partial Frame with Cast-in-Place Concrete Shear Walls	C4	High-rise					
			Mid-rise					
Frame-core wall structure	C5	High-rise						
		High-rise						
Tube-in-tube structure	C6	Super high-rise						
		High-rise						
Slab-column-wall structure	C7	Super high-rise						
		Mid-rise						

Table 2 (continued)

Material	Building typology	Code	Height level	Irregularities		Code level	SPI	Building actuality
				Horizontal	Vertical			
Steel (S)	Steel moment frame	S1	High-rise					
			Mid-rise					
			High-rise					
	Steel braced frame	S2	High-rise					
				Super high-rise				
				Low-rise				
Steel light frame	Steel Frame with Un-reinforced Masonry Infill Walls	S3	High-rise					
		S4	High-rise					
Steel Frame with Cast-in-Place Concrete Shear Walls		S5	Super high-rise					
			High-rise					
Steel and RC composite system		S6	Super high-rise					
			High-rise					
Wooden (W)	Wood structures	W	Super high-rise					
			Low-rise					

Table 3 Ground motion records selected from China Earthquake Networks Center

Event	Year	Station name	Recording direction	M_w	PGA (cm/s ²)
Gansu	2003	062MIL	NS	6.1	331
Gansu	2003	062MIL	UD	6.1	333
Lijiang	1996	294	EW	7.0	178
Lijiang	1996	294	NS	7.0	137
Longling	1976	30	NS	6.2	155
Longling	1976	30	WE	6.2	181
Puer	2007	053JZX	NS	6.4	406
Puer	2007	053PDH	NS	6.4	432
Wenchuan	2008	051JYD	NS	8.0	459
Wenchuan	2008	051SFB	EW	8.0	556

3.3.2 Fragility analysis

The methods to derive fragility functions include empirical, expert opinion-based, analytical, and hybrid method (Ahmad et al. 2010; Ptilakis and Argyroudis 2014). Due to the aforementioned local characteristic of structures in China, different methods were adopted to create the corresponding fragility functions. Sun and Zhang (2012) used the observed data of buildings damaged by 2008 Wenchuan earthquake to generate the fragility matrix. Empirical methods take advantage of real earthquake disaster and experiments while cannot fully consider important factors including different building attributes and randomness in ground motion due to the limited data gathered so far. Considering these deficiencies, most fragility functions are built following analytical method (Wu et al. 2012; Jiang et al. 2015).

In the present study, the fragility functions of adobe, stone, and unreinforced brick masonry are built based on statistics of observed damage from past earthquakes and experiments (Sun and Zhang 2012; Zhang 2010). For other kind of building typology, numerical simulations are performed to derive the fragility functions. Firstly, multiple index buildings that can represent the class of proposed building typology are designed and numerical modeled. A set of 22 far field ground motion records are selected from PEER NGA strong ground motions database as recommended by a series reports (FEMA P-695 2009; D'Ayala et al. 2014) and a set of 10 ground motion records are selected from China Earthquake Networks Center (CENC, <http://data.earthquake.cn>). The details of Chinese ground motion set are summarized in Table 3. Incremental dynamic analyses (IDA) are carried out, where each record is scaled up until the collapse of the building occurs. According to the results of IDA, the correlation coefficients between the ground motion intensity measures (IM) and the structure damage measure (DM) were calculated. Then the fragility function can be obtained as follow.

In the above procedures, two main issues related to the fragility curves are selections of an appropriate seismic IM as well as a structure DM. An optimal IM can characterize the strong ground motion and even correlate with the structural response (NGI 2013). Due to the majority and diversity of buildings in urban areas, it is difficult to select a unified structure-specific IM. The structure-independent IMs should be considered such as peak ground acceleration (PGA) and peak ground velocity (PGV). In addition, PGA is also consistent with the ground motion attenuation models of China. Therefore, PGA is adopted to

develop the fragility curves. As suggested by CCSDB (NSPRC 2010), the maximum peak inter-story drift over the height of building, denoted θ_{\max} , is chosen as the damage measure to reflect the damage degree of the components as well as the structure. This parameter is suitable for the urban-scale seismic fragility estimation since it can be widely retrieved from both the experimental observations and numerical simulations. The damage states are divided as none damage (ND), slight damage (SD), moderate damage (MD), extensive damage (ED), and complete damage (CD) following the definitions provided in code of Classification of earthquake damage to buildings and special structures (NSPRC 2009).

3.4 Loss assessment

Seismic risk is represented by the probabilistic physical damage of an individual building while considering local hazard, vulnerability, and inventory. Based on the physical damage results, both direct economic losses and number of casualties are calculated.

With the rapid urbanization of China, wealth is mostly centered in urban regions. The affiliated value of a building is more apparent, which represents a large proportion of its replacement costs. To assess economic loss more precisely, a direct economic loss model is proposed based on the model of Sun and Chen (2009), which considers the structure loss, decoration loss, and content loss. In addition, the differences of economic level in urban areas are considered. The proposed direct economic loss model is developed as follows:

$$L_{\text{total}} = \alpha(L_S + L_D + L_C) \quad (1)$$

$$L_S = \sum_{i=1}^n \sum_{j=1}^5 M_i \cdot P(DS = ds_j) \cdot \mu_{ds_j}^s \quad (2)$$

$$L_D = \gamma_1 \cdot \gamma_2 \cdot \gamma_3 \sum_{i=1}^n \sum_{j=1}^5 \eta_1 \cdot M_i \cdot P(DS = ds_j) \cdot \mu_{ds_j}^d \quad (3)$$

$$L_C = \sum_{i=1}^n \sum_{j=1}^5 \eta_2 \cdot M_i \cdot P(DS = ds_j) \cdot \mu_{ds_j}^c \quad (4)$$

where L_{total} is the expected total direct economic loss for any geographical unit; α is the loss multiplier accounting for the ignored losses (e.g., natural environment loss), suggested as 1.0 to 1.3; L_S , L_D , and L_C are the structure loss, decoration loss, and content loss, respectively; $P(DS = ds_j)$ is the probability for damage state ds_j to be incurred on an individual building in an earthquake; M_i is the replacement cost for structure i , which is equal to the product of replacement cost per floor area and total floor area; $\mu_{ds_j}^s$, $\mu_{ds_j}^d$ and $\mu_{ds_j}^c$ are the loss ratios for damage state ds_j on the structure, decoration and content, respectively; γ_1 , γ_2 and γ_3 are the decoration loss correction factors considering the economic developmental variety, building occupancy, and decoration level, respectively; η_1 is the ratio of decoration cost to the structure replacement cost; and η_2 is the ratio of the content cost to the structure replacement cost.

As the result of observations of past major historical earthquakes in China, several casualty models have been developed considering seismic intensity, earthquake time, and population density parameters. However, the uneven distribution of population caused by the

occupancy levels and economic status is not considered in these models. By considering damage probability, occupancy, population density, structure type and earthquake time, a new casualty model is proposed that can estimate the number of deaths, severe injuries and minor injuries. As described in Eq. 5.

$$N_{s,i} = \sum_{j=1}^n N_j = \alpha \cdot \gamma \cdot \eta \cdot N_0 \sum_{j=1}^n A_j P_j \quad (5)$$

where $N_{s,i}$ is the total number of casualties in severity level i , $i=1$ to 3, where 1—minor injury, 2—severe injury, and 3—death; N_j is the number of individual building j in severity level i ; α is the regional multiplier accounting for the population density variation between the different regions; γ is population density correction factor in different occupancy levels; η is the people indoor rate in different occupancy levels at different earthquake times; N_0 is the number of people per floor area; A is the total floor area; and P_j is the mean damage ratio (e.g., death ratio is given as Eq. 6), which relates to the damage state and the casualty ratio in different damage states.

$$P_j = P_{l=1}P_{d=1} + P_{l=2}P_{d=2} + P_{l=3}P_{d=3} + P_{l=4}P_{d=4} + P_{l=5}P_{d=5} \quad (6)$$

where P_l is the probabilities in damage state l ; $l=1$ to 5, which represents none, slight, moderate, extensive, and complete, respectively. P_d is casualty rate in damage state d ; $d=1$ to 5, with the same values for 1 to 5 as previously outlined for l .

4 Application and discussion

4.1 General description

Xi'an is an earthquake-prone region due to its tectonic setting. According to the latest Seismic ground motion parameters zonation map of China (NSPRC 2015), Xi'an is located in seismic fortification intensity zone VIII (0.20 g). Baqiao, with a population of 500,000, is one of the oldest districts in Xi'an, Shaanxi province, which is located in the middle of Guanzhong basin. With an area of 332 km², the district is divided into nine sub-district regions (including 33 communities and 226 administrative villages) as shown in Fig. 6. Baqiao is an old industrial district known for its textile industry. Its buildings are typically composed of adobe and brick masonry. However, with the development of urbanization and the recession of the textile industry, some older buildings have been demolished and replaced by new reinforced concrete shear wall buildings, especially industrial buildings.

4.2 Structure classification

Considering the efficiency of field survey, a detailed survey and spot check of buildings were separately carried out in Baqiao. The detailed survey, considered the differences in individual buildings, was conducted in the urban and urban-rural areas. Information about structure type, condition, construction year, occupancy, floor area, and other parameters can be obtained from this survey. Spot checks, however, were used for the buildings with only minor differences (e.g., for rural areas). The parameters of construction year, height, occupancy, structure type, and regional difference were considered in the spot check. 61,625 buildings were checked in Baqiao with 28,969 building data

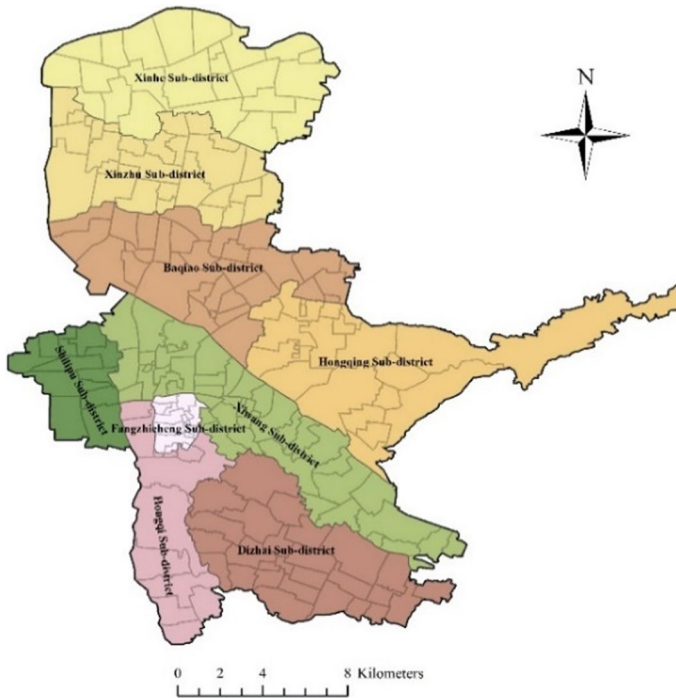


Fig. 6 Overview of Baqiao District. The district is divided into nine sub-district regions: Xinhe, Xinzhu, Baqiao, Shilipu, Fangzhicheng, Xiwang, Hongqing, Hongqi, and Dizhai

collected in total. The entire data field work lasted for more than 10 months. According to structure type, construction year, occupancy, and number of stories, the statistical results of different building distribution are shown in Fig. 7.

As shown in Fig. 7a, buildings in the case study area are mainly composed of reinforced brick masonry (69.0%) and unreinforced brick masonry (25.1%). Bottom frame structures are usually used for commercial due to large space at the bottom. Considering the relatively high cost of construction, RC frame structures and RC shear wall structures are rarely constructed compared to reinforced brick masonry buildings. With the development of urbanization, RC shear wall structures and RC frame with cast-in-place concrete shear walls structures are commonly used for high-rise buildings. According to the year of construction, 82% of surveyed buildings were constructed after 1990 following the introduction of earthquake-resistant design principles in 1989 CCSD (NSPRC 1989). Since 1990, reinforced brick masonry buildings have rapidly expanded in China; at the same time, unreinforced brick masonry stocks have been restricted in cities, which largely limits such construction to rural and undeveloped areas (Fig. 7b). Statistics from the survey show that the buildings are predominately built for residential use, with only a few for commercial (0.38%) and education (0.37%) (Fig. 7c). As seen from the Fig. 7d, the buildings are almost low-rise (85.5%) and mid-rise (14.1%). The number of RC frame structures are mainly from 4 to 9, and the number distribution of RC shear wall are all above 12 in the range of high-rise.

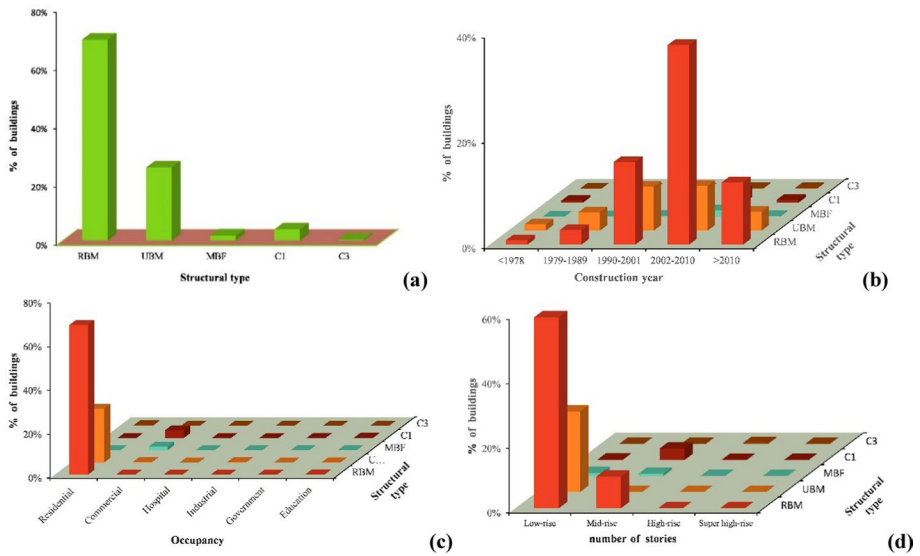



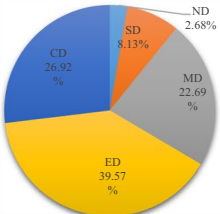

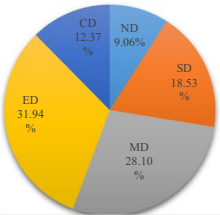

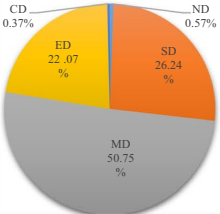

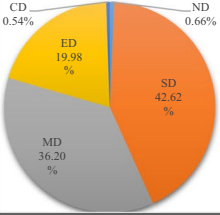

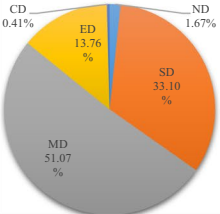

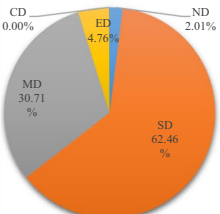
Fig. 7 Distribution of buildings in detailed survey area. From left to right and top to bottom: **a** structure type **b** construction year **c** occupancy, and **d** number of stories

According to the field survey data, the buildings are classified into six types based on construction material and structural system. Reinforced brick masonry (RBM), unreinforced brick masonry (UBM), masonry with bottom frame (MBF), concrete moment frame (C1), and concrete shear wall structures (C3) are built in the detailed survey area, and adobe (A) and unreinforced brick masonry (UBM) are in the spot check area. A qualitative description of building features is provided in the following and the photos of typical building types are shown in Table 4.

Adobe masonry (A) Adobe masonry is built with sun-dried earth brick in mud mortar or constructed mud walls with horizontal wood elements. Considering the advantages of easily availability material, simplified construction, and low cost, adobe masonry structures are widely constructed in rural areas of China. Unfortunately, those structures are highly vulnerable in earthquakes. Statistics show that adobe structures are severely damaged in earthquake intensity VII, and completely damaged and collapsed in earthquake intensity above VIII. Adobe structures in Baqiao were typically built in the undeveloped administrative villages or neighborhood communities before 1980 and are typically self-constructed with wooden roofs (Table 4). The characteristics of adobe are as follows: (1) the adobe is constructed with low strength and viscosity of mud; (2) many cracks can be seen in adobe walls because of the uneven foundation settlement; (3) the configurations of adobe are mostly arbitrary and unreasonable especially in the self-constructed buildings, which could lead to out-of-plane failure or torsional damage.

Unreinforced brick masonry (UBM) Unreinforced brick masonry buildings (UBM) are constructed without appropriate seismic measures (i.e., ring beams and structural columns) as shown in Table 4. The UBM buildings in Baqiao are mainly located in administrative villages and are almost exclusively low rise (1–3 stories). The survey indicates that the overall seismic performance of the UBM structure is poor due to the lack of effective seismic measures. Also, the floors are precast concrete slabs, and the roofs are mostly wooden structures. The phenomenon of foundation settlement and wall-cracks increase the

Table 4 Characteristics of building typology in Baqiao district

Building typology	Photo	Descriptions of typical seismic damage	Percentages of five damage states												
A		Partial or complete collapse is common due to lack of effective lateral resistance and bearing system. Out of plane failure of adobe walls and rapid developed shear cracks are general reasons for adobe structures to experience severe damage.	 <table border="1"> <tr><th>Damage State</th><th>Percentage</th></tr> <tr><td>ND</td><td>2.68%</td></tr> <tr><td>SD</td><td>8.13%</td></tr> <tr><td>MD</td><td>22.69%</td></tr> <tr><td>ED</td><td>39.57%</td></tr> <tr><td>CD</td><td>26.92%</td></tr> </table>	Damage State	Percentage	ND	2.68%	SD	8.13%	MD	22.69%	ED	39.57%	CD	26.92%
Damage State	Percentage														
ND	2.68%														
SD	8.13%														
MD	22.69%														
ED	39.57%														
CD	26.92%														
UBM		Diagonal cracking forms in walls between openings where the extremely fragile part of the building are. Some walls failed out-of-plane failure patterns due to lack of connections between walls.	 <table border="1"> <tr><th>Damage State</th><th>Percentage</th></tr> <tr><td>ND</td><td>9.06%</td></tr> <tr><td>SD</td><td>18.53%</td></tr> <tr><td>MD</td><td>28.10%</td></tr> <tr><td>ED</td><td>31.94%</td></tr> <tr><td>CD</td><td>12.37%</td></tr> </table>	Damage State	Percentage	ND	9.06%	SD	18.53%	MD	28.10%	ED	31.94%	CD	12.37%
Damage State	Percentage														
ND	9.06%														
SD	18.53%														
MD	28.10%														
ED	31.94%														
CD	12.37%														
RBM		Most of the damage concentrates at the lower part of the structure while the upper floors only experience slight damage. Shear cracks appear in walls, while the whole performance is much better than UBM due to the good integrity.	 <table border="1"> <tr><th>Damage State</th><th>Percentage</th></tr> <tr><td>ND</td><td>0.57%</td></tr> <tr><td>SD</td><td>26.24%</td></tr> <tr><td>MD</td><td>50.75%</td></tr> <tr><td>ED</td><td>22.07%</td></tr> <tr><td>CD</td><td>0.37%</td></tr> </table>	Damage State	Percentage	ND	0.57%	SD	26.24%	MD	50.75%	ED	22.07%	CD	0.37%
Damage State	Percentage														
ND	0.57%														
SD	26.24%														
MD	50.75%														
ED	22.07%														
CD	0.37%														
MBF		The lateral stiffness variation in the vertical is the main reason for the phenomenon that the second floors always have more severe damage than the first ones. In extreme cases, the second layer can disappear.	 <table border="1"> <tr><th>Damage State</th><th>Percentage</th></tr> <tr><td>ND</td><td>0.66%</td></tr> <tr><td>SD</td><td>42.62%</td></tr> <tr><td>MD</td><td>36.20%</td></tr> <tr><td>ED</td><td>19.98%</td></tr> <tr><td>CD</td><td>0.54%</td></tr> </table>	Damage State	Percentage	ND	0.66%	SD	42.62%	MD	36.20%	ED	19.98%	CD	0.54%
Damage State	Percentage														
ND	0.66%														
SD	42.62%														
MD	36.20%														
ED	19.98%														
CD	0.54%														
C1		Plastic hinges form more in the column ends than in the beam ends, which is deviated from the expected failure mechanism. Also, the short columns with shear failure can be found due to inappropriate layout of infill walls and openings.	 <table border="1"> <tr><th>Damage State</th><th>Percentage</th></tr> <tr><td>ND</td><td>1.67%</td></tr> <tr><td>SD</td><td>33.10%</td></tr> <tr><td>MD</td><td>51.07%</td></tr> <tr><td>ED</td><td>13.76%</td></tr> <tr><td>CD</td><td>0.41%</td></tr> </table>	Damage State	Percentage	ND	1.67%	SD	33.10%	MD	51.07%	ED	13.76%	CD	0.41%
Damage State	Percentage														
ND	1.67%														
SD	33.10%														
MD	51.07%														
ED	13.76%														
CD	0.41%														
C3		Horizontal and diagonal cracks can be found in shear walls which compose highly effective lateral resistance system. The non-structural component damage is slighter comparing to the RC frame structure.	 <table border="1"> <tr><th>Damage State</th><th>Percentage</th></tr> <tr><td>ND</td><td>2.01%</td></tr> <tr><td>SD</td><td>62.46%</td></tr> <tr><td>MD</td><td>30.71%</td></tr> <tr><td>ED</td><td>4.76%</td></tr> <tr><td>CD</td><td>0.00%</td></tr> </table>	Damage State	Percentage	ND	2.01%	SD	62.46%	MD	30.71%	ED	4.76%	CD	0.00%
Damage State	Percentage														
ND	2.01%														
SD	62.46%														
MD	30.71%														
ED	4.76%														
CD	0.00%														

potential risk to seismic effects as well. These buildings were mainly constructed in the 1960s without seismic retrofitting. Even new self-constructed buildings ignore the current seismic design codes.

Reinforced brick masonry (RBM) Different from adobe and UBM buildings, the ring beams and structural concrete columns can be observed in the RBM buildings. In Baqiao, buildings constructed after 1990 are typically with three to six stories and are structurally sound and follow good construction practice (Table 4). In addition, after the Tangshan earthquake in 1976, many unreinforced brick masonry buildings constructed between 1950 and 1970 with no seismic design code were retrofitted with the ring beam and structural concrete columns. After retrofitting, these buildings are considered as RBMs.

Masonry with bottom frame (MBF) Masonry with bottom frame is a special structure type with a reinforced concrete frame for the first floor and a masonry or concrete block structure at upper floors (Gong et al. 2015). The framing system of MBF consists of moment resisting frame and brick wall system. Because the material and mechanical properties are different, the seismic performance of the MBF is more complex. Many MBF structures can be founded in Baqiao including multi-storey residential, hotel, and office buildings with first floor restaurants (Table 4).

RC frame structures (C1) Most RC frame structures in Baqiao are designed and constructed following national seismic design codes, and mainly found in the developed, high population density areas due to its relatively high costs in construction. RC frame structures are designed to have the failure mechanism of strong-column and weak beam, and they are expected to have good seismic performance. These buildings are used for commercial and administration. The buildings are typically four to nine stories high and were constructed after 1990 (Table 4).

Concrete shear wall structures (C3) A concrete shear wall structure is a special structure that adopts the reinforced concrete walls to resist vertical and horizontal seismic force. Due to the perfect seismic performance with large lateral stiffness, these structures are commonly used for high-rise buildings. In recent years, with the development of urbanization in Baqiao, some older buildings have been demolished and replaced by new reinforced concrete shear wall buildings. Located along the Canhe River, these high-rise/super-high-rise buildings are mainly used for residential and commercial (Table 4).

4.3 Earthquake loss assessment

4.3.1 Seismic hazard analysis

The classical deterministic seismic hazard analysis is carried out based on the historical earthquake. 1556 Huaxian M_s 8.0 earthquake (located at 109.7E Longitude and 34.5 N Latitude in Shaanxi province) are used as scenario earthquake. The earthquake caused huge destruction, and killed more than 830,000 people (Lv et al. 2014). The main seismogenic structure includes Huashan piedmont fault, Weihe fault, and Weinan front fault. The seismic intensity of meizoseismal areas was XI as shown in Fig. 8.

Baqiao is located in the southwest of Huaxian city, approximately 70 km from the epicenter. Historical statistics show that the Huaxian earthquake caused a seismic intensity of IX in Baqiao. Seismic hazard analysis is conducted based on the ground motion attenuation model and the characteristics of site amplification. The former has obvious regional characteristics depending on the properties of source, propagation medium, and site condition, etc. (Hu 1990). The present study used the ground motion attenuation model developed by

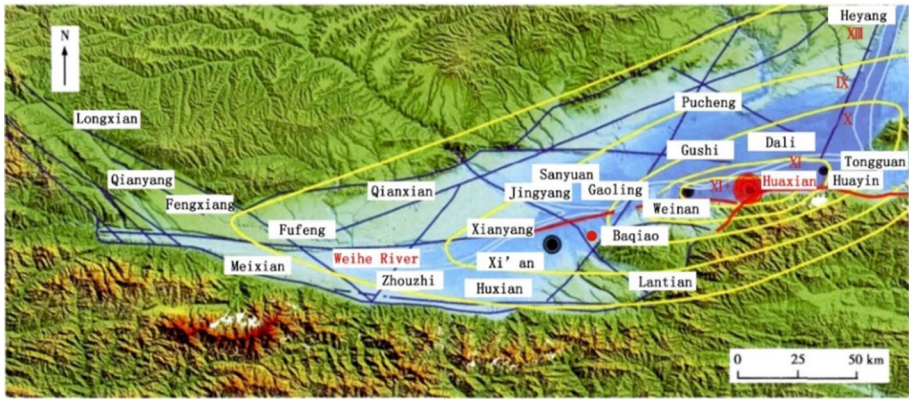


Fig. 8 Earthquake intensity map and seismogenic faults for the Huaxian earthquake from Lv et al. (2014)

Yu and Wang (2003), and the equations for major axis and minor axis are shown respectively as follow:

$$\lg Y = 2.206 + 0.532M - 1.954\lg(R + 2.018e^{0.406M}) \tag{7}$$

$$\lg Y = 1.010 + 0.501M - 1.441\lg(R + 0.340e^{0.521M}) \tag{8}$$

where Y represents the horizontal component of PGA in g ; M represents the surface wave magnitude; and R represents the hypocentral distance (unit: km).

The impact of site conditions on the propagation of seismic waves is a complicated problem, which manifests as a strong amplification or reduction effect on different frequency components of ground motions as well as the PGA (Konakli and Der Kiureghian 2012). This impact is considered by adjusting PGA with the site amplification factor, k_{sp} . The site amplification model proposed by Chen and Duan (2013) is utilized because the model is built based on the borehole data in Xi'an area. The model is shown as follow:

$$k_{sp} = \exp(1.660 - 0.412 \lg H - 0.368 \lg V_s) \tag{9}$$

where H represents the soil thickness (unit: m) and V_s represents the mean value of shear wave velocity (unit: m/s). Both the parameters can be obtained from the geological survey report from local government (Xi'an Geophysical Exploration Center 2011).

The seismic hazard analysis is carried out using the above equations and the theory in Sect. 3.1, which are integrated in the tool—CEDLAS. Considering the differences in the site conditions of the Baqiao district, the whole area has been resampled on a uniform grid of 0.5 km × 0.5 km, which results in a database of 92,597 geocells. The results of PGA map of Baqiao are shown in Fig. 9. The value of PGA from 0.3 to 0.5 g as shown in Fig. 9 is in accordance with the intensity distribution given by Seismic ground motion parameters zonation map of China (NSPRC 2015).

4.3.2 Fragility functions for case study structures

As mentioned in Sect. 4.2, the buildings in Baqiao are classified by structure type, construction year, occupancy, and number of stories. Since seismic precautionary intensity of

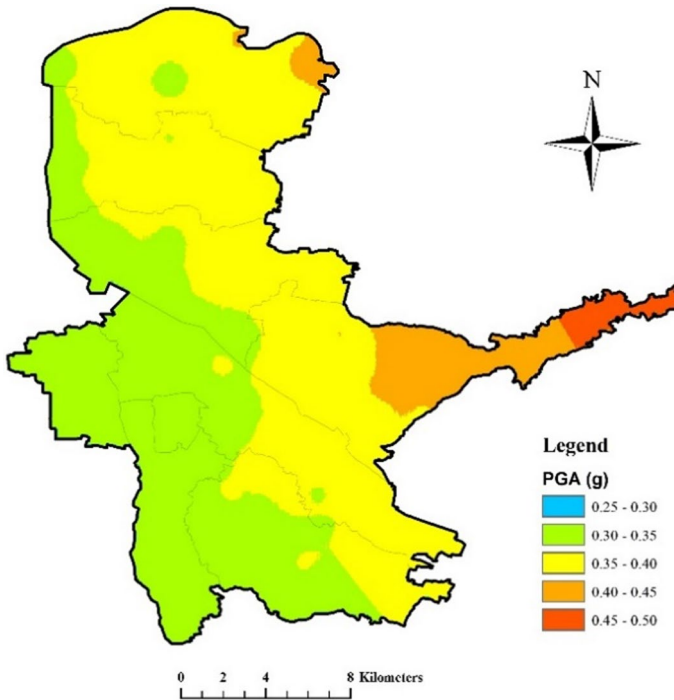


Fig. 9 The peak acceleration map of Baqiao calculated using Huaxian earthquake

Baqiao is VIII (0.20 g), the fragility curves are determined considering only the structure type, number of stories, and seismic design code. The fragility functions for the case study structures can be derived using the methodology proposed in Sect. 3.3.2 and the results are shown in Fig. 10.

4.3.3 Damage analysis

The damage analysis for the case study area under the 1556 Huaxian earthquake is investigated. The seismic peak ground acceleration distribution, building inventory, and fragility curves are integrated as described in Fig. 11. The probability for different damage states to be incurred on individual buildings in Huaxian earthquake can be seen in the bar chart below (Fig. 11). The detailed percentages of five failure states for different building typologies are calculated as shown in Table 4. Meanwhile, according to the structural engineering reconnaissance of past earthquakes (Sun and Zhang 2012; Gong et al. 2015), typical seismic damage of corresponding buildings are summarized in Table 4. It appears that adobe structures have the most severe damage as reflected by their highest percentage of complete damage (26.92%) and extensive damage (39.57%). Comparing with unreinforced brick masonry buildings, the seismic performance of reinforced brick masonry buildings raised obviously due to the mandated use of special details. The seismic performance of MBF is similar to RBM. It's noted that the ratios of complete damage of RC frame structures and shear wall structures are both low, especially the latter ones because they all built following

Fig. 10 Fragility functions for building typologies in Baqiao. From left to right and top to bottom: **a** A, Low-rise, Pre-code, **b** UBM, Low-rise, Pre-code, **c** RBM, Low-rise, All codes, **d** RBM, Mid-rise, All codes, **e** C1, Low-rise, All codes, **f** C1, Mid-rise, All codes, **g** C1, High-rise, High-code, **h** C3, High-rise, High-code. SD-slight damage, MD-moderate damage, ED-extensive damage, CD-complete damage

the latest two versions of seismic codes. This manifests that current seismic codes are effective in preventing structural collapse in strong earthquakes.

4.3.4 Loss assessment

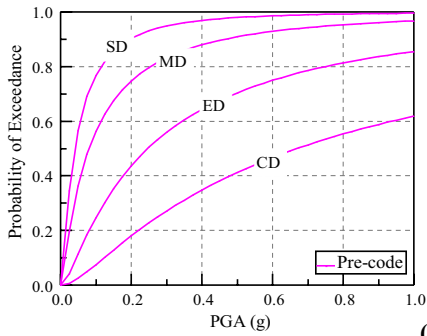
According to the construction industry statistical yearbook in China from 2004 to 2013, a reasonable building replacement cost using the construction completion value and floor area in different year throughout all the provinces is obtained. Due to the complex tectonic with collapsible loess covered in Baqiao, the loss multiplier α is 1.1 accounting for the natural environment loss. The direct economic loss (e.g., structure loss, decoration loss, content loss, and total loss) can be seen in Fig. 12. It is noted that Fig. 12 is based on the results of average predictions. The corresponding upper and lower bounds of economic losses are shown in Table 5 to illustrate the possible range of losses in Baqiao district.

As shown in Fig. 12a, most structure losses occurred in neighborhood communities and administrative villages in Fangzhicheng and Xiwang. The buildings, with high occupancy are mostly older brick masonry. After the 1976 Tangshan earthquake, most of UBM buildings were retrofitted by setting ring beams and structural columns. However, there are still some unreinforced brick masonry and self-constructed buildings found in this area, especially in Xiwang. The decoration loss can be seen from Fig. 12b, with the higher losses concentrated in the Fangzhicheng sub-district region. The economic characteristic is uneven due to the variation in decoration factor. High and moderate decoration factors are found in the densely populated Fangzhicheng sub-district regions, while low decoration factors are found in undeveloped areas. In general, the content losses are directly related to the economics of the region. However, the field survey shows that in some areas, the buildings with poor seismic resistance performance have high content values, which may increase in the direct economic losses (Fig. 12c). The total direct economic losses are shown in Fig. 12d, which are the sum of structure losses, decoration losses, and content losses as shown in Fig. 12d. The higher losses are mostly concentrated in Fangzhicheng, Hongqi, Xiwang, and Baqiao sub-district regions, where the proportions of losses caused by decoration and content damage are larger than these proportions in other regions.

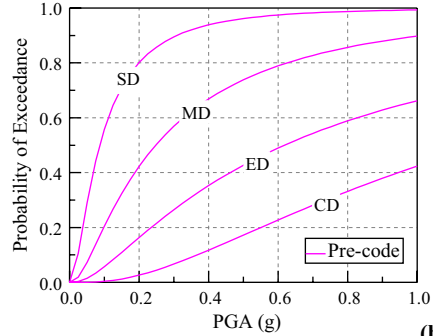
The population distribution in Baqiao is highly uneven, with the greatest population concentrated in the Fangzhicheng and Shilipu sub-district regions. The regional multiplier α is set to 0.8 in view of the population density variation among different regions. The number of people per floor area N_0 and population density correction factor γ in different occupancy classes are carried out based on the census data and questionnaire survey as shown in Table 6.

In order to obtain the occupancy rate in different types of buildings at different times of a day, a questionnaire survey was conducted among Baqiao residents. The analysis from 1200 questionnaires is shown in Table 7.

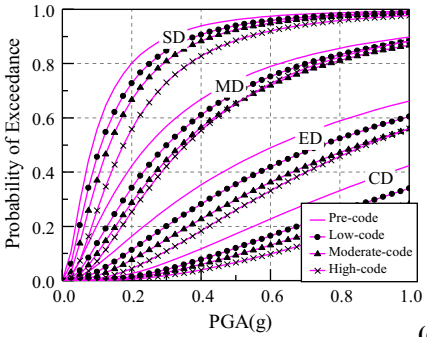
Based on the proposed casualty model (Eq. 5) and above parameters, the average casualties are calculated as shown in Fig. 13. Detailed numbers of casualties are summarized in Table 8 including the upper and lower bounds of predictions. The majority of casualties occurred in large, populated areas, such as Fangzhicheng, Shilipu, and



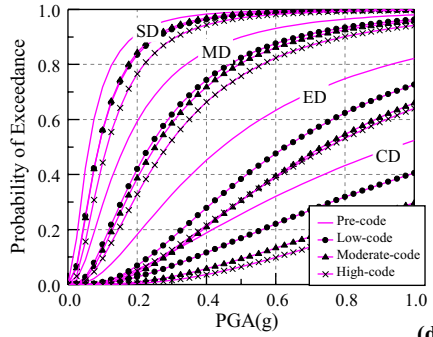
(a)



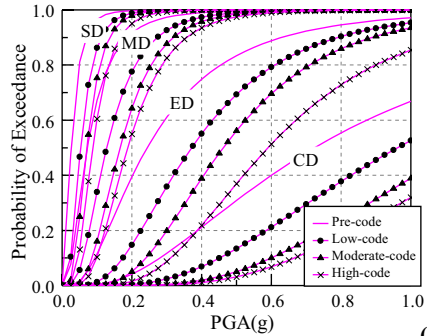
(b)



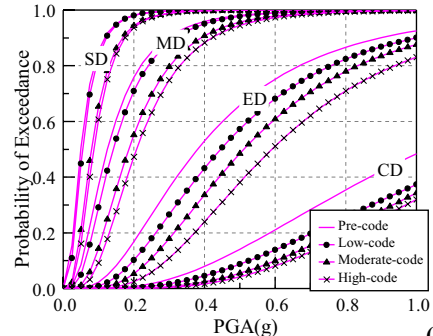
(c)



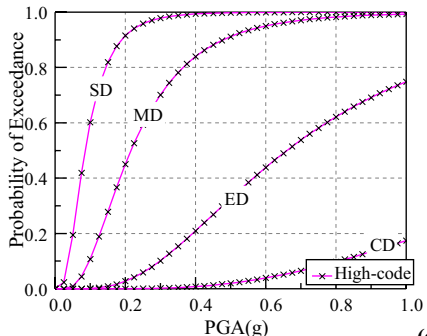
(d)



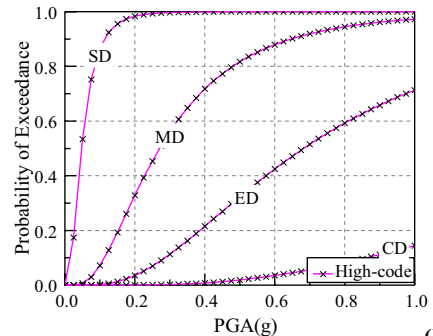
(e)



(f)



(g)



(h)

Xiwang sub-district regions. The scenario earthquake happens at night (22:00–07:00) most of the residents would be sleeping, and the number of casualties would be higher than if the earthquake occurred during the day. The ground motion intensity decreased from northeast to southwest (Fig. 9). In the northeast, most areas are sparsely populated farmland and mountains, thus resulting in relatively fewer casualties. However, the southwest area is more densely populated with many unreinforced brick masonry buildings, thereby resulting in large majority of casualties. More casualties are found in the Fangzhicheng, Xiwang, and Hongqing sub-district regions which are similar to higher economic loss concentrated regions.

According to the estimation results of earthquake loss assessment in Baqiao, the losses are mainly distributed in Fangzhicheng and Xiwang sub-district regions. These regions have a higher economic level and a high building and population density. However, in some areas, buildings are constructed in close proximity and do not meet the seismic design code. Therefore, when an earthquake occurs, these buildings can also be damaged and destroyed by fire and debris. These secondary disasters greatly affect rescue activities. In other words, the method may underestimate the resulting earthquake disaster losses without considering secondary disasters. It is noted that the predicted range of casualties varies significantly, especially for the number of death. This is because there are many factors affecting casualties, and the uncertainty of each factor is relatively large due to incomplete statistical data.

4.4 Discussions

4.4.1 Discussion on the results of loss assessment

The overall loss assessment results of Baqiao district show that the socio-economic impacts are high due to the seismic prone characteristic and amount of pre-code buildings. It is noted that the government is pushing the program of retrofitting UBM buildings. To demonstrate if retrofitting may help the region in risk mitigation, all UBM buildings are replaced with RBM buildings in the CEDLAS, and another simulation is carried out. Two simulation results of loss assessment are archived in Appendix Table A for comparing the effect of retrofitting.

As presented in Table A, a slight decrease (1.8%) of direct economic loss is observed in Baqiao district after retrofitting. It is noted that the economic impact is not as obvious as expected. This mainly because the structure, decoration, and content costs of UBM are higher than those of RBM in the case of the same floor area. Meanwhile, the structural damage is certainly less after retrofitting, resulting in a mild decrease in economic loss. However, the estimated casualties are much lower after retrofitting. In Hongqing sub-district region, the number of death decreases from 142 before retrofitting to 71 after retrofitting. Despite the accuracy of the presented method to show the impacts of retrofitting UBM can be improved, the results are enough to illustrate the urgency and effectiveness of implementing retrofitting programs.

4.4.2 Discussion on the limits of proposed earthquake loss model

The proposed methodology is used for the assessment of urban-scale earthquake losses in China. However, to avoid the expensive computational cost, some effects that may have

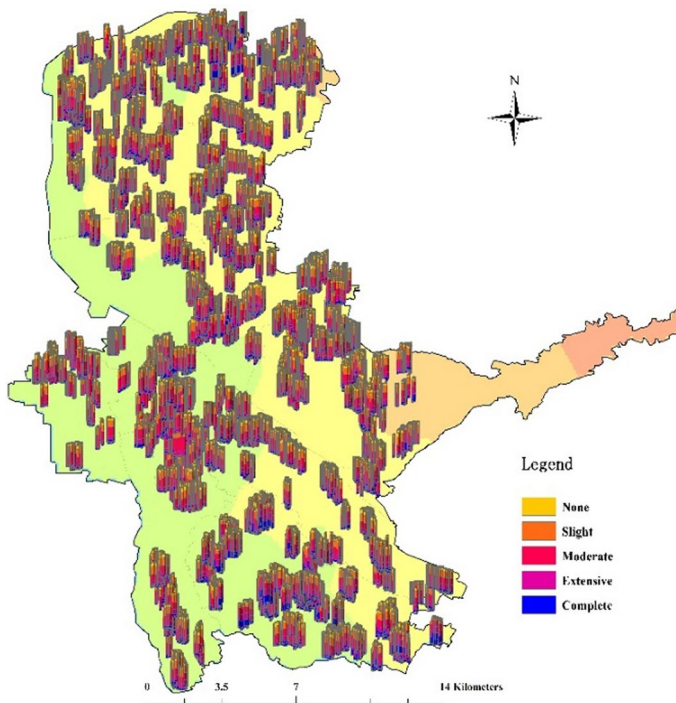


Fig. 11 Probability of structure damage in bar chart

impacts on the final results of losses are simplified considered and discussed in the following. (1) In the procedure of seismic hazard analysis, site effects are included using an equation to amplify the parameter of ground motion. Recently, more ground shaking modelling techniques have been developed to directly reflect the spatial variability in ground motions. For example, Xiong et al. (2020) considered a coupled site-city effect for seismic damage simulation on a region-scale. (2) In the procedure of seismic fragility analysis, different building typologies are included while the corresponding numerical modeling techniques can still be improved for some typical buildings. For example, in-plane and out-of-plane behavior would be coupled under multi-directional seismic action (Ahmad et al. 2012; Al Hanoun et al. 2019) while only the in-plane mechanism is considered in the modeling of masonry walls.

5 Conclusions and future developments

This paper proposes an integrated framework for earthquake loss assessment in China. This new assessment methodology can account for Chinese special characteristics. Several key components are included: a new data collection method is devised using a mobile GIS-based field collection tool that can effectively collect detailed building inventory; a hierarchical, detailed, and extensible building typology was proposed to assess the fragility of buildings based on 2010 CCSDB; and a new economic loss model and casualties model are developed for assessing individual buildings to estimate the loss and number of casualties.

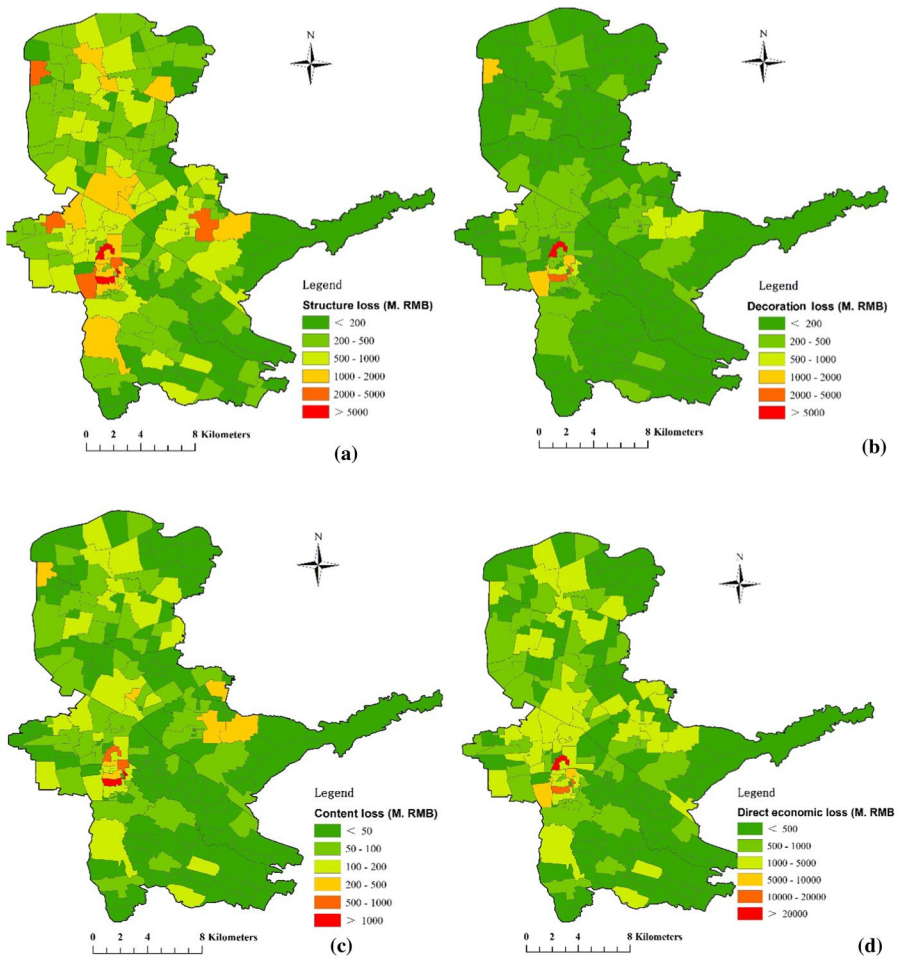


Fig. 12 Direct economic loss assessment in Baqiao at neighborhood community and administrative village level. From left to right and top to bottom: **a** structure loss, **b** decoration loss, **c** content loss, and **d** direct economic loss (in million RMB)

Table 5 The range of economic losses in Baqiao (in billion RMB)

Economic loss	Structure loss	Decoration loss	Content loss	Direct economic loss
Average value	1274.7	319.6	169.4	1763.7
Range	[667.5, 1713.9]	[301.6, 624.7]	[91.3, 171.4]	[1060.4, 2510.0]

Table 6 The number of people per floor area N_0 and population density correction factor γ in different occupancy classes

Occupancy	Suggested value of N_0	Range value of γ	Suggested value of γ
Residential	0.015 people per m ²	0.3–0.8	0.7
Commercial		2.5–3.8	3.0
Industrial		–	0.7
Education		3.9–7.4	5.0
Hospital		0.5–3.0	1.7
Government		0.5–2.5	1.5

Table 7 The occupancy rate of Baqiao in different occupancy classes at different times

Time	Residential	Commercial	Industrial	Education	Hospital	Government
22:00–07:00	1.0	0.1	0	0	0.78	0
07:00–09:00	0.68	0.4	0.4	0.7	0.60	0.1
09:00–11:00	0.43	1.0	1.0	0.95	0.72	1.0
11:00–13:00	0.75	0.4	0.5	0.7	0.50	0.3
13:00–17:00	0.45	1.0	1.0	0.95	0.90	0.9
17:00–19:00	0.67	0.4	0.5	0.5	0.84	0.2
19:00–22:00	0.87	0.1	0.3	0.3	0.78	0.1

Baqiao district is used as a case study and the economic losses and number of casualties are estimated. The results of retrofitting of UBM buildings in Baqiao district are presented. The case study can provide useful information for urban disaster risk assessment and mitigation. Using the proposed methodology, it is possible to accomplish the following: (1) scientifically evaluate the degree of damage to buildings in future earthquakes and reduce the socio-economic losses, (2) suggest mitigation measures for decision-makers, and (3) assist insurance departments in estimating insurance rates.

This earthquake loss assessment framework is a complex project that integrates the components of seismic hazard, inventory, fragility, and loss assessment. Based on the methodologies, the stand-alone system CEDLAS is developed in ArcGIS Engine and the “.NET” framework environment. Because some functions of the system are still under testing, the system is currently not publicly available. With successful development, it not only provides a tool for earthquake loss assessment, but also integrates the latest research findings, accurate data and new methodologies for risk management and loss assessment. Further development will primarily concentrate on the following aspects: (1) implementing recovery decision making by considering reinforcement methods and cost–benefit analysis, (2) improving the accuracy and efficiency of data collection, (3) improving the function module and testing the stability of overall system, and (4) integrating the latest research findings and new methodologies into the tool CEDLAS to improve the applicability to other countries.

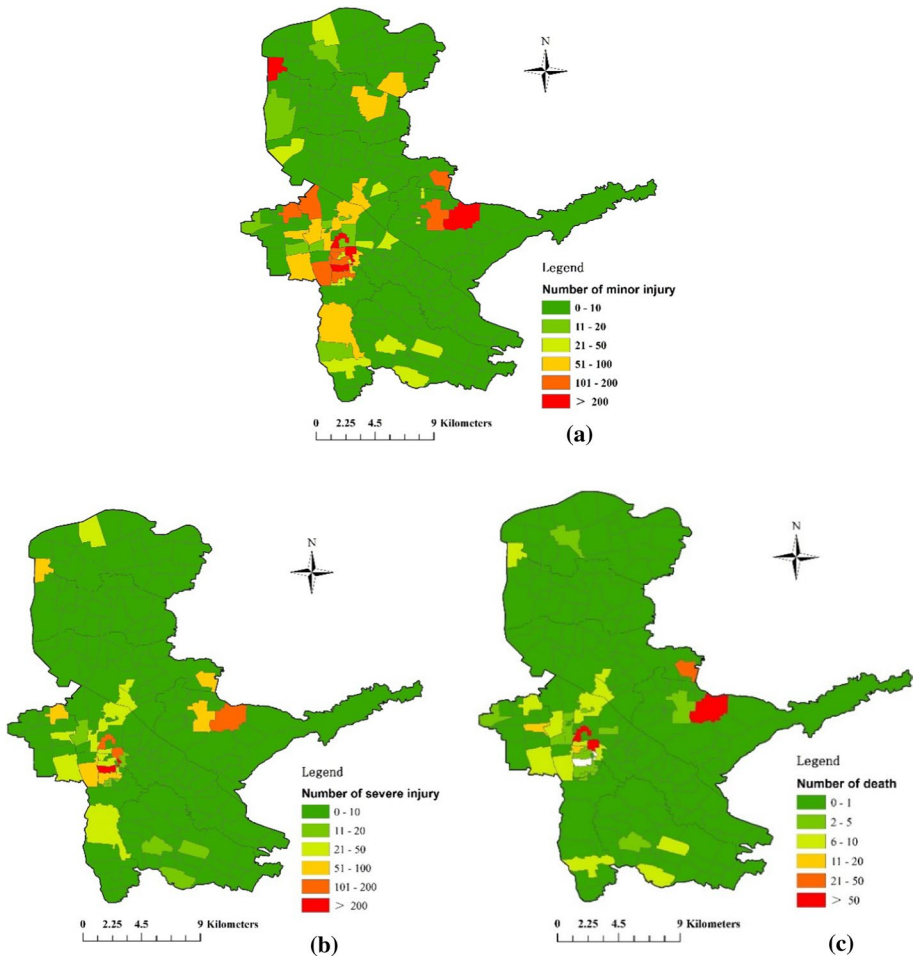


Fig. 13 The distribution of casualty estimation in Baqiao at neighborhood community and administrative village level. From left to right and top to bottom: number of minor injury, number of severe injury, and number of death

Table 8 The range of casualties in Baqiao

Number of casualties	Minor injury	Severe injury	Death
Average number	17,605	5248	1201
Range	[12031, 31337]	[2301, 9708]	[487, 2936]

Acknowledgements The research described in this paper was financed by the National Natural Science Foundation of China with Grant No. 51678475 and the Research Fund of Shaanxi Province in China with Grant No. 2017ZDXM-SF-093. Part of the basic data was provided by the Earthquake Administration of Xi'an and the Government of Baqiao District. This support is greatly acknowledged.

Appendix

See Table 9.

Table 9 Comparisons of loss assessment in sub-districts of Baqiao

Sub-district	Xiawang	Baqiao	Xinhe	Xinzhu	Shilipu	Dizhai	Hong-qing	Fang-zhicheng	Hongqi	Total
Direct economic loss (in billion RMB)										
Structure										
W/O	281.2	156.4	103.2	156.3	76.5	58.3	114.8	239.0	89.0	1274.7
W/	281.3	156.5	102.7	155.7	76.5	58.1	113.8	239.0	88.9	1272.5
R_1 (%)	0.02	0.07	-0.51	-0.42	0.00	-0.34	-0.82	0.01	-0.13	-0.18
Decoration										
W/O	86.4	37.2	23.7	34.8	19.3	11.4	26.3	56.9	23.6	319.6
W/	86.5	37.3	23.9	34.9	19.3	11.4	26.5	56.9	23.6	320.3
R_2 (%)	0.12	0.31	0.75	0.20	0.00	0.42	0.54	0.02	0.06	0.21
Content										
W/O	25.3	26.8	15.1	21.8	10.9	7.9	14.5	36.4	10.8	169.4
W/	25.2	26.8	14.7	21.4	10.9	7.7	13.9	36.4	10.7	167.8
R_3 (%)	-0.38	0.12	-2.73	-1.70	-0.01	-1.82	-3.83	-0.04	-0.56	-0.96
Total										
W/O	393.0	220.4	142.0	212.9	106.6	77.6	155.6	332.4	123.4	1763.7
W/	393.0	220.6	141.2	211.9	106.6	77.3	154.2	332.4	123.2	1760.5
R_4 (%)	0.02	0.12	-0.54	-0.45	0.00	-0.38	-0.87	0.00	-0.13	-0.18
Number of casualties										
Minor injury										
W/O	2534	2829	1668	2279	970	1104	1838	3352	1031	17,605
W/	2328	2610	1208	1878	970	960	1318	3310	971	15,553
R_5 (%)	-8.13	-7.74	-27.58	-17.60	0.00	-13.04	-28.29	-1.25	-5.82	-11.66
Severe injury										
W/O	699	837	555	672	249	413	595	931	297	5248
W/	596	722	327	479	249	342	341	909	268	4233
R_6 (%)	-14.74	-13.74	-41.08	-28.72	0.00	-17.19	-42.69	-2.36	-9.76	-19.34

Table 9 (continued)

Sub-district	Xiwang	Baqiao	Xinhe	Xinzhu	Shilipu	Dizhai	Hong-qing	Fang-zhicheng	Hongqi	Total
Death										
W/O	152	192	134	152	51	107	142	204	67	1201
W/	123	159	70	97	51	87	71	198	58	914
R_7 (%)	- 19.08	- 17.19	- 47.76	- 36.18	0.00	- 18.69	- 50.00	- 2.94	- 13.43	- 23.90

R_n is the changing ration of different loss contents, which is calculated as dividing the value of variation in corresponding loss content by the original value; $n = 1$ to 7, which represents structure loss, decoration loss, content loss, total loss, minor injury, severe injury, and death, respectively. W/O means without retrofitting measures, and W/ means with retrofitting measures

References

- Ahmad N, Crowley H, Pinho R et al (2010) Displacement-based earthquake loss assessment of masonry buildings in Mansehra city. *Pak J Earthq Eng* 14(S1):1–37
- Ahmad N, Ali Q, Ashraf M et al (2012) Seismic vulnerability of the Himalayan half-dressed rubble stone masonry structures, experimental and analytical studies. *Nat Hazards Earth Syst Sci* 12(11):3441–3454
- Ahmad N, Ali Q, Crowley H, Rui P (2014) Earthquake loss estimation of residential buildings in Pakistan. *Nat Hazards* 73(3):1889–1955
- Ahmad N, Shahzad A, Ali Q et al (2018) Seismic fragility functions for code compliant and non-compliant RC SMRF structures in Pakistan. *Bull Earthq Eng* 16(10):4675–4703
- Al Hanoun MH, Abrahamczyk L, Schwarz J (2019) Macromodeling of in-and out-of-plane behavior of unreinforced masonry infill walls. *Bull Earthq Eng* 17(1):519–535
- Annuziato A, Gadenz S, Galliano DA et al (2010) Field tracking tool: a collaborative framework from the field to the decision makers. *Geographic information and cartography for risk and crisis management*. Springer, Berlin, pp 287–303
- ATC-13 (1985) Earthquake damage evaluation data for California. Applied Technology Council, Redwood City
- Baker JW (2008) An introduction to probabilistic seismic hazard analysis (PSHA). White Paper, Version 1.3. <http://www.stanford.edu/~bakerjw/publications.html>. Accessed 2 May 2013
- Bal IE, Crowley H, Pinho R et al (2008) Detailed assessment of structural characteristics of Turkish RC building stock for loss assessment models. *Soil Dyn Earthq Eng* 28(10):914–932
- Brzev S, Scawthorn C, Charleson AW et al (2013) GEM building taxonomy. GEM technical report, Version 1.0.0. <https://pubs.er.usgs.gov/publication/70045104>. Accessed 16 Mar 2017
- Chen DM, Duan R (2013) Amplification effects of site conditions on ground peak acceleration. *J Earthq Eng Eng Vib* 33(1):24–30 (in Chinese)
- China Earthquake Networks Center, National Earthquake Data Center. <http://data.earthquake.cn>
- Choun YS, Elnashai AS (2010) A simplified framework for probabilistic earthquake loss estimation. *Probab Eng Mech* 25(4):355–364
- Coburn A, Spence R (2003) Earthquake protection. Wiley, Hoboken
- Cornell CA (1968) Engineering seismic risk analysis. *Bull Seismol Soc Am* 58(5):1583–1606
- D'Ayala D, Meslem A, Vamvastikos D, Porter K, Rossetto T, Crowley H, Silva V (2014) Guidelines for analytical vulnerability assessment of low/mid-rise Buildings—Methodology. Vulnerability Global Component project. Available from: <https://www.nexus.globalquakemodel.org/gem-vulnerability/posts/>
- Duzgun HSB, Yucemen MS, Kalaycioglu HS et al (2011) An integrated earthquake vulnerability assessment framework for urban areas. *Nat Hazards* 59(2):917–947
- Ellingwood BR, Wen YK (2005) Risk-benefit-based design decisions for low-probability/high consequence earthquake events in mid-America. *Prog Struct Mater Eng* 7(2):56–70
- ESRI (2010) ArcGIS. Version 10.1. Redlands, United States
- Fan W, Du WH, Wang XJ et al (2011) Seismic motion attenuation relations in Shaanxi areas. *Earthq Eng Eng Vib* 31(2):47–54
- Federal Emergency Management Agency (2002) Rapid visual screening of buildings for potential seismic hazards: a handbook, 2nd edn. FEMA, Washington
- Federal Emergency Management Agency (FEMA) (2012a) Multi-hazard loss estimation methodology, earthquake model, HAZUS–MH 2.1 technical manual. Washington, DC
- Federal Emergency Management Agency (FEMA) (2012b) Multi-hazard loss estimation methodology HAZUS–MH 2.1 advanced engineering building module (AEBM) technical and user's manual. Washington, DC
- Federal Emergency Management Agency-National Institute of Building Sciences (FEMA-NIBS) (1997) Earthquake loss estimation methodology–HAZUS99. Washington, DC
- Gao X, Zhong Y, Chen D (1989) A method on prediction of seismic damage for reinforced concrete frames. *Build Sci* 01:16–23
- Global Earthquake Model (GEM) (2013). <http://www.globalquakemodel.org>
- Gong M, Lin S, Sun J et al (2015) Seismic intensity map and typical structural damage of 2010 Ms 7.1 Yushu earthquake in China. *Nat Hazards* 77(2):847–866
- Haldar P, Singh Y, Lang DH, Paul DK (2013) Comparison of seismic risk assessment based on macroseismic intensity and spectrum approaches using 'SeisVARA.' *Soil Dyn Earthq Eng* 48:267–281
- Hu YX (1990) Comprehensive probability method for the seismic risk analysis. Earthquake Press, Beijing (in Chinese)
- IDCT (2011) <http://www.globalquakemodel.org/resources/use-and-share/tools-apps/>

- Jaiswal K, Wald D, Porter K (2010) A global building inventory for earthquake loss estimation and risk management. *Earthq Spectra* 26(3):731–748
- Jeon JS (2013) Aftershock vulnerability assessment of damaged reinforced concrete buildings in California. Georgia Institute of Technology, Atlanta
- Jiang HJ, Liu XJ, Hu L (2015) Seismic fragility assessment of RC frame-shear wall structures designed according to the current Chinese seismic design code. *J Asian Archit Build Eng* 14(2):459–466
- Joint Research Centre (JRC) (2013) Development of inventory datasets through remote sensing and direct observation data for earthquake loss estimation. SYNER-G technical report
- Ketner KB (2008) Creating a global building inventory for earthquake loss assessment and risk management. U.S. geological Survey.
- Konakli K, Der Kiureghian A (2012) Simulation of spatially varying ground motions including incoherence, wave-passage and differential site-response effects. *Earthq Eng Struct Dyn* 41(3):495–513
- Lin SL, Li J, Elnashai AS, Spencer BF Jr (2012) NEES integrated seismic risk assessment framework (NISRAF). *Soil Dyn Earthq Eng* 42:219–228
- Liu JW, Wang ZM, Xie FR, Lv YJ (2013) Seismic hazard assessment for greater North China from historical intensity observations. *Eng Geol* 164:117–130
- Long L, Zheng SS, Zhang YX et al (2020) CEDLES: a framework for plugin-based applications for earthquake risk prediction and loss assessment. *Nat Hazards* 103:531–556
- Lv Y, Dong Y, Feng XJ et al (2014) Characteristics of geological relics due to 1556 Huaxian great earthquakes in Guanzhong area of Shaanxi province, China. *J Eng Geol* 22(2):300–308 (in Chinese)
- MAEviz (2018) <http://rcp.ncsa.uiuc.edu/maeviz/about.html>
- Mansour AK, Romdhane NB, Boukadi N (2013) An inventory of buildings in the city of Tunis and an assessment of their vulnerability. *Bull Earthq Eng* 11(5):1563–1583
- Mansouri B, Amini-Hosseini K (2014) Development of residential building stock and population databases and modeling the residential occupancy rate for Iran. *Nat Hazards Rev* 15(1):88–94
- Mansouri B, Ghafory-Ashtiany M, Amini-Hosseini K et al (2010) Building seismic loss model for Tehran. *Earthq Spectra* 26(1):153–168
- McGuire RK (2008) Probabilistic seismic hazard analysis: early history. *Earthq Eng Struct Dyn* 37:329–338
- Molina S, Lang DH, Lindholm CD (2010) SELENA—an open-source tool for seismic risk and loss assessment using a logic tree computation procedure. *Comput Geosci* 36(3):257–269
- National Bureau of Statistics of the People's Republic of China (NBSPRC) (2015) The People's Republic of China national economic and social development statistical bulletin in 2014. http://www.stats.gov.cn/tjsj/zxfb/201502/t20150226_685799.html (in Chinese)
- National Standard of People's Republic of China (NSPRC) (1979) Chinese aseismic code of industrial and civil buildings (TJ11-78). Ministry of Construction of People's Republic of China, Beijing (in Chinese)
- National Standard of People's Republic of China (NSPRC) (1989) Chinese code for seismic design of buildings (GBJ11-89). Ministry of Construction of People's Republic of China, Beijing (in Chinese)
- National Standard of People's Republic of China (NSPRC) (2001) Chinese code for seismic design of buildings (GB50011-2001). Ministry of Construction of People's Republic of China, Beijing (in Chinese)
- National Standard of People's Republic of China (NSPRC) (2009) Classification of earthquake damage to buildings and special structures (GB/T24335-2009). Ministry of Construction of People's Republic of China, Beijing (in Chinese)
- National Standard of People's Republic of China (NSPRC) (2010) Chinese code for seismic design of buildings (GB50011-2010). Ministry of Construction of People's Republic of China, Beijing (in Chinese)
- National Standard of People's Republic of China (NSPRC) (2015) Seismic ground motion parameter zonation map of China, GB 18306–2015. China Standard Publishing House, Beijing (in Chinese)
- Norwegian Geotechnical Institute (NGI) (2013) SYNER-G fragility curves for all elements at risk. SYNER-G technical report
- Pagani M, Monelli D, Weatherill G, Danciu L, Crowley H (2014) Openquake engine: an open hazard (and risk) software for the global earthquake model. *Seismol Res Lett* 85(3):692–702
- Pan H, Gao MT, Xie FR (2013) The earthquake activity model and seismicity parameters in the new seismic hazard map of China. *Technol Earthq Disaster Prev* 8(1):11–23 (in Chinese)
- Pitilakis K, Argyroudis S (2014) Introduction to the applications of the SYNER-G methodology and tools. In: SYNER-G: systemic seismic vulnerability and risk assessment of complex urban, utility, lifeline systems and critical facilities. Springer, pp 185–198
- Applied Technology Council (2009) Quantification of building seismic performance factors (FEMA P-695), Washington, DC

- Sahar L, Muthukumar S, French SP (2010) Using aerial imagery and GIS in automated building footprint extraction and shape recognition for earthquake risk assessment of urban inventories. *IEEE Trans Geosci Remote Sens* 48(9):3511–3520
- Seismic Vulnerability Assessment Project Group (SVAPG) (2013) Seismic vulnerability assessment of building types in India, Technical Document on Typology of Buildings in India
- Silva V, Crowley H, Pagani M, Monelli D, Rui P (2014) Development of the openquake engine, the global earthquake model's open-source software for seismic risk assessment. *Nat Hazards* 72(3):1–19
- Spence KSR (2011) Mapping urban building stocks for vulnerability assessment-preliminary results. *Int J Digit Earth* 4(1):117–130
- Sun BT, Chen HF (2009) Urban building loss assessment method considering the decoration damage due to earthquake. *J Earthq Eng Eng Vib* 29(5):164–169
- Sun, BT, Chen HF, Zhong YZ (2012) Development of earthquake disaster loss estimation in China. In: *Proceedings of the 15th world conference on earthquake engineering, 2012*
- Sun BT, Zhang GX (2012) Statistical analysis of the seismic vulnerability of various types of building structures in Wenchuan M8.0 earthquake. *China Civ Eng J* 45(5):26–30 (in Chinese)
- SYNER-G (2013) <http://www.vce.at/SYNER-G/>
- Wang JP, Taheri H (2014) Seismic hazard assessment of the Tehran region. *Nat Hazards Rev* 15:121–127
- Wang YY (2008) Lessons learnt from building damages in the Wenchuan earthquake: seismic concept design of buildings. *J Build Struct* 4(4):20–25 (in Chinese)
- Wieland M, Pittore M, Parolai S et al (2012) Estimating building inventory for rapid seismic vulnerability assessment: towards an integrated approach based on multi-source imaging. *Soil Dyn Earthq Eng* 36:70–83
- Wu D, Tesfamariam S, Stiemi SF, Qin D (2012) Seismic fragility assessment of RC frame structure designed according to modern Chinese code for seismic design of buildings. *Earthq Eng Eng Vib* 11(3):331–342
- Xi'an Geophysical Exploration Center, Xi'an Earthquake Administration (2011) Seismic ground motion parameters zonation map of Xi'an
- Xiong C, Huang J, Lu X (2020) Framework for city-scale building seismic resilience simulation and repair scheduling with labor constraints driven by time-history analysis. *Comput Aided Civ Infrastruct Eng* 35(4):322–341
- Xu Z, Lu X, Guan H, Han B, Ren A (2014) Seismic damage simulation in urban areas based on a high-fidelity structural model and a physics engine. *Nat Hazards* 71(3):1679–1693
- Yin ZQ (1995) Method for earthquake disaster predicting and loss assessment. Earthquake Press, Beijing (in Chinese)
- Yu YX, Li SY, Xiao L (2013) Development of ground motion attenuation relations for the new seismic hazard map of China. *Technol Earthq Disaster Prev* 8(1):24–33 (in Chinese)
- Yu YX, Wang SY (2003) Attenuation relations for horizontal peak ground acceleration and response spectrum in Eastern and Western China. *Technol Earthq Disaster Prev* 1(3):206–217 (in Chinese)
- Zhang GX (2010) Two methods for earthquake damage prediction of building groups base on multi-parameters. Master dissertation, Institute of Engineering Mechanics, China Earthquake Administration (in Chinese)

Publisher's Note Springer Nature remains neutral with regard to jurisdictional claims in published maps and institutional affiliations.